DALTON
FULL PAPER

Control of the hapticity of pyridine-2-thiolate ligands in rhenium(V) oxo complexes†

António Paulo, Ângela Domingos and Isabel Santos *

Departamento de Química, Estrada Nacional 10, ITN, 2686-593 Sacavém Codex, Portugal.
E-mail: isantos@itn1.itn.pt

Received 22nd July 1999, Accepted 17th September 1999

Treatment of $[ReO\{\kappa^3-B(pz)_4\}(OMe)_2]$ **1** with pyridine-2-thiol ligands led to $[ReO\{\kappa^2-B(pz)_4\}(\kappa^2-Spy^*)(OMe)]$ (Spy* = 2-SC_5H_4N **2** or 2-$SC_5H_3NSiMe_3$-3 **3**) or $[ReO\{\kappa^3-B(pz)_4\}(\kappa^1-2-SC_5H_4N)_2]$ **4**, depending on the reaction conditions. Complexes **2** and **3** reacted with trimethylsilyl chloride yielding $[ReO\{\kappa^3-B(pz)_4\}(\kappa^1-2-SC_5H_4N)Cl]\cdot HCl$ **6** and $[ReO\{\kappa^3-B(pz)_4\}Cl_2]$, respectively. The characterization of the new compounds involves IR and ^1H NMR spectroscopies, and X-ray diffraction analysis for **3**, **4** and **6**.

Introduction

In recent years, rhenium–thiolate chemistry has received considerable attention, mainly due to the potential usefulness of some rhenium(V)-thiolate complexes as models for the development of diagnostic (^{99m}Tc) or therapeutic (^{186,188}Re) radiopharmaceuticals.[1–4] In particular, pyridine-2-thiolate ligands gave an important contribution to the expansion of rhenium-thiolate chemistry, due to their co-ordination versatility.[4–6]

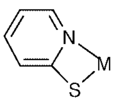
I

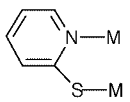
II

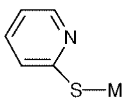
III

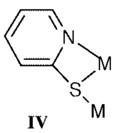
IV

Our group has been exploring the chemistry of rhenium(V) oxo complexes with tetrakis(pyrazolyl)borate (B(pz)$_4$) and has shown that an easy control of the co-ordination mode (κ^2 or κ^3) of this ligand can be achieved by using $[ReO\{\kappa^3-B(pz)_4\}(OMe)_2]$ **1** as starting material.[7–12] Following these studies, we decided to investigate the chemistry of complex **1** with pyridine-2-thiolate ligands presenting different electronic and/or stereochemical properties.

In this paper we report reactions of complex **1** with pyridine-2-thiol and 3-trimethylsilylpyridine-2-thiol, which allowed the synthesis and characterization of $[ReO\{\kappa^2-B(pz)_4\}(\kappa^2-Spy^*)(OMe)]$ (Spy* = 2-SC_5H_4N **2** or 2-$SC_5H_3NSiMe_3$-3 **3**) and $[ReO\{\kappa^3-B(pz)_4\}(\kappa^1-2-SC_5H_4N)_2]$ **4**, depending on the reaction conditions. We also describe the synthesis and characterization of the derivative $[ReO\{\kappa^3-B(pz)_4\}(\kappa^1-2-SC_5H_4N)Cl]\cdot HCl$ **6** obtained by treating **2** with an excess of trimethylsilyl chloride. Complexes **2**–**6** were characterized by analytical and spectroscopic methods and, in the case of **3**, **4** and **6**, by X-ray crystallography.

Experimental

General procedures

The reactions were carried out under a nitrogen atmosphere using standard Schlenk techniques or dry glove-boxes. Solvents were dried, degassed and distilled prior to use, according to described procedures. The compounds $[ReO\{\kappa^3-B(pz)_4\}(OMe)_2]$ **1**, $[\{ReO(\mu-O)[\kappa^3-B(pz)_4]\}_2]$ and 2-$HSC_5H_3NSiMe_3$-3 were prepared as described.[9,13] The other chemicals were used as purchased.

The ^1H NMR spectra were recorded on a Varian Unity 300 MHz spectrometer, referenced with the residual solvent resonances relative to tetramethylsilane, in $CDCl_3$, CD_2Cl_2 or toluene-d$_8$. The coupling constants for the protons of B(pz)$_4$ varied between 1.8 and 2.4 Hz, as observed previously, and are omitted for clarity.[7–12] The IR spectra were recorded as KBr pellets on a Perkin-Elmer 577 spectrometer. In the spectra of complexes **2**–**6** the bands due to B(pz)$_4$ appear at wavelengths almost superimposable with the ones previously described for rhenium(V) oxo complexes containing κ^2-B(pz)$_4$ or κ^3-B(pz)$_4$.[7–12] Carbon, hydrogen and nitrogen analyses were performed on a Perkin-Elmer automatic analyser.

Syntheses

$[ReO\{\kappa^2-B(pz)_4\}(\kappa^2-Spy^*)(OMe)]$ (Spy* = 2-SC_5H_4N 2 or 2-$SC_5H_3NSiMe_3$-3 3). To a blue solution of $[ReO\{\kappa^3-B(pz)_4\}(OMe)_2]$ **1** (200 mg, 0.36 mmol) in dichloromethane was added an equimolar amount of pyridine-2-thiol or 3-trimethylsilylpyridine-2-thiol dissolved in the minimum volume of dichloromethane. Each reaction mixture was allowed to react at room temperature for 2 h, yielding clear yellow-brown solutions. After removal of the solvent and washing with *n*-hexane, 130 mg (0.20 mmol) of **2** (58%) or 155 mg (0.22 mmol) of **3** (62%) were obtained as microcrystalline yellow-brown solids.

Compound **2**. Calc. for $C_{18}H_{19}BN_9O_2ReS$: C, 34.7; H, 3.1; N, 20.3. Found: C, 34.9; H, 3.0; N, 19.9%. IR (cm^{-1}): 945s (ν(Re–O)) and 514s (ν(Re–OMe)). ^1H NMR (300 MHz, $CDCl_3$): δ 2.74 (3 H, s, OCH_3), 6.16 (1 H, t, H(4)), 6.22 (1 H, t, H(4)), 6.55 (1 + 1 H, br, H(4)), 6.69 (1 H, d, H(3/5)), 6.75 (1 H, d, H(3/5)), 7.06 (1 H, t, J = 6.6, Ph, Spy*), 7.15 (1 H, d, J = 8.1, Ph, Spy*), 7.31 (1 H, d, H(3/5)), 7.41 (1 H, d, H(3/5)), 7.56 (1 H, d, J = 5.4 Hz, Ph, Spy*), 7.65 (1 H, br, H(3/5)), 7.71–7.77 (1 + 1 H, br, H(3/5) + Ph, Spy*), 8.05 (1 H, d, H(3/5)) and 8.20 (1 H, d, H(3/5)).

Compound **3**. Calc. for $C_{21}H_{27}BN_9O_2ReSSi$: C, 36.3; H, 3.9; N, 18.1. Found: C, 36.4; H, 3.9; N, 18.0%. IR (cm^{-1}): 945s (ν(Re–O)) and 510m (ν(Re–OMe)). ^1H NMR (300 MHz, $CDCl_3$): δ 0.42 (9 H, s, $Si(CH_3)_3$), 2.74 (3 H, s, OCH_3), 6.15 (1 H, t, H(4)), 6.22 (1 H, t, H(4)), 6.54 (1 + 1 H, br, H(4)), 6.69 (1 H, d, H(3/5)), 6.77 (1 H, d, H(3/5)), 7.06 (1 H, dd, J = 7.4, 5.6 Ph, Spy*), 7.31 (1 H, d, H(3/5)), 7.41 (1 H, d, H(3/5)), 7.65 (1 H, d, H(3/5)), 7.74 (1 H, d, H(3/5)), 7.85 (1 H, dd, J = 8.3, 1.8, Ph, Spy*), 8.04 (1 H, d, H(3/5)), 8.23 (1 H, d, H(3/5)) and 8.54 (1 H, dd, J = 5.7, 1.8 Hz, Ph, Spy*).

---

† *Supplementary data available*: rotatable 3-D crystal structure diagram in CHIME format. See http://www.rsc.org/suppdata/dt/1999/3735/

[ReO{κ^3-B(pz)$_4$}(κ^1-2-SC$_5$H$_4$N)$_2$] 4. *Method 1.* The complex [ReO{κ^3-B(pz)$_4$}(OMe)$_2$] **1** (100 mg, 0.18 mmol) and pyridine-2-thiol (41 mg, 0.37 mmol) were dissolved in toluene (20 ml) and the resulting blue solution was heated at reflux for 2 h, turning to yellow-brown. After concentration under vacuum followed by addition of *n*-hexane a yellow-brown microcrystalline solid precipitated which was formulated as **4**. This solid was vacuum dried, after filtration and washing with *n*-hexane, yielding 90 mg (0.13 mmol) of **4** (71%).

Method 2. To a suspension of the dimer [{ReO(μ-O)-[κ^3-B(pz)$_4$]}$_2$] (100 mg, 0.2 mmol of Re) in dichloromethane was added pyridine-2-thiol (45 mg, 0.4 mmol) dissolved in the minimum volume of dichloromethane. The reaction occurred almost immediately with formation of a clear and brownish solution. After stirring at room temperature for 1 h the solvent was removed under vacuum and a brown residue was obtained. The ^{1}H NMR analysis of this residue showed the presence of complex **4** and of another species. Complex **4** was extracted with toluene and by recrystallization from toluene–hexane brownish crystals were obtained (40%). The X-ray analysis of these crystals showed the presence of one molecule of pyridine-2-thiol as solvate. The fraction insoluble in toluene was recrystallized from CH$_2$Cl$_2$–hexane, precipitating a salmon solid that, even after several recrystallizations, was always slightly contaminated with a minor non identified species. However, this salmon solid was tentatively formulated as "[{ReO[κ^2-B(pz)$_4$](κ^2-2-SC$_5$H$_4$N)$_2$}$_2$(μ-O)]" **5** based on IR and ^{1}H NMR spectroscopies (see Results and discussion).

Compound **4**. Calc. for C$_{22}$H$_{20}$BN$_{10}$OReS$_2$: C, 37.7; H, 2.9; N, 20.0. Found: C, 37.8; H, 2.8; N, 19.8%. IR (cm^{-1}): 965s (ν(Re–O)). ^{1}H NMR (300 MHz): δ (CD$_2$Cl$_2$, 20 °C), 6.10 (1 H, br, H(4)), 6.22 (2 H, br, H(4)), 6.63 (1 H, br, H(4)), 6.77 (2 H, br, Ph, Spy*), 6.99 (2 H, t, J = 5.9, Ph, Spy*), 7.35 (2 H, t, J = 6.9, Ph, Spy*), 7.75 (3 H, br, H(3/5)), 7.92 (4 H, d, H(3/5)), 8.17 (1 H, br, H(3/5)) and 8.48 (2 H, d, J = 3.9 Hz, Ph, Spy*); (CD$_2$Cl$_2$, −80 °C) 5.44 (1 H, br), 5.88 (1 H, br), 6.08 (1 H, br), 6.53 (1 H, br), 6.60 (1 H, br), 6.84 (1 + 1 H, br), 6.94 (1 H, br), 7.21 (1 H, br), 7.50 (1 H, br), 7.77 (1 + 1+1 H, br), 7.81 (1 H, br), 7.89 (1 H, br), 7.94 (1 H, br), 7.99 (1 H, br), 8.38 (1 H, br), 8.54 (1 H, br) and 8.66 (1 H, br); (toluene-d$_8$, 60 °C), 5.70 (4 H, br, H(4)), 6.48 (2 H, t, J = 6.0, Ph, Spy*), 6.88 (2 H, t, J = 11.4, Ph, Spy*), 7.02 (2 H, t, J = 11.4, Ph, Spy*), 7.45 (4 H, br, H(3/5)), 7.99 (4 H, br, H(3/5)) and 8.30 (2 H, d, J = 4.5 Hz, Ph, Spy*).

Compound **5**. IR (cm^{-1}): 970w (ν(Re–O)) and 680s (ν(Re–O–Re)). ^{1}H NMR (300 MHz, CDCl$_3$): δ 5.97 (1 H, t, H(4)), 6.25 (1 H, t, H(4)), 6.44 (1 H, t, H(4)), 6.51 (1 H, d, H(3/5)), 6.57 (1 H, d, H(3/5)), 6.63 (1 H, t, H(4)), 6.67 (1 H, d, H(3/5)), 6.82 (1 H, d, H(3/5)), 6.92 (1 H, d, H(3/5)), 6.98 (1 H, t, J = 5.4, Ph, Spy*), 7.22 (1 H, d, J = 8.4, Ph, Spy*), 7.43 (1 H, d, H(3/5)), 7.59 (1 H, d, H(3/5)), 7.82 (1 H, t, J = 8.0, Ph, Spy*), 7.86 (1 H, d, H(3/5)) and 8.07 (1 H, d, J = 3.6 Hz, Ph, Spy*).

[ReO{κ^3-B(pz)$_4$}(κ^1-2-SC$_5$H$_4$N)Cl]·HCl 6. To a yellow-brown solution of complex **2** in dichloromethane an excess (10:1 molar ratio) of trimethylsilyl chloride was added. The reaction mixture was allowed to react overnight at room temperature, giving a green solution. Complex **6** was recovered by removal of the solvent followed by washing with toluene. Starting from 100 mg (0.15 mmol) of **2** were obtained 80 mg of **6** (80%) as a microcrystalline green solid. Calc. for C$_{17}$H$_{17}$BCl$_2$N$_9$OReS: C, 30.8; H, 2.6; N, 19.0. Found: C, 31.1; H, 2.4; N, 18.5%. IR (cm^{-1}): 963s (ν(Re–O)) and 335m (ν(Re–Cl)). ^{1}H NMR (300 MHz, CDCl$_3$): δ 6.13 (1 H, t, H(4)), 6.51 (1 H, t, H(4)), 6.57 (1 H, br, H(4)), 6.66 (1 H, br, H(4)), 7.65 (1 H, m, Ph, Spy*), 7.72–7.74 (1 + 1 H, m, H(3/5)), 7.92 (1 H, d, H(3/5)), 7.97–8.02 (1 + 1+1 H, m, H(3/5) + Ph, Spy*), 8.15 (1 H, d, H(3/5)), 8.21–8.27 (1 + 1 H, m, H(3/5) + Ph, Spy*), 8.43 (1 H, d, H(3/5)), 8.82 (1 H, d, J = 4.8 Hz, Ph, Spy*) and 18.46 (1 H, br, NH, Spy*).

X-Ray crystallographic analysis

X-Ray data were collected from yellow-brown crystals of complex **3**, from brownish crystals of **4** and from green crystals of **6** obtained, respectively, by recrystallization from methanol–*n*-hexane, toluene–*n*-hexane and from dichloromethane–toluene. Data were collected on an Enraf-Nonius CAD-4 diffractometer with graphite-monochromated Mo-Kα radiation, using an ω-2θ scan mode. The crystal data are summarized in Table 1.

The data were corrected[14] for Lorentz-polarization effects and for absorption (Ψ scans). The crystal of complex **3** did not provide a good quality data set but the structure was determined unambiguously, although displaying an unusually short Re–O(2) bond. The heavy atom positions were located by Patterson methods using SHELXS 86.[15] The remaining atoms were located in successive Fourier-difference maps and refined by least-squares refinements on F^2 using SHELXL 93.[16] The structural analysis revealed one molecule of pyridine-2-thiol per asymmetric unit for complex **4** and in the case of **6** one molecule of CH$_2$Cl$_2$ per asymmetric unit. All the non-hydrogen atoms were refined with anisotropic thermal motion parameters. The pyridinium hydrogens, for complex **6** and for pyridine-2-thiol of crystallization in **4**, were located from the difference maps and allowed to refine isotropically. The contributions of the other hydrogen atoms were included in calculated positions. For **3** the highest residual electron density was 2.98 e Å^{-3}, 1.02 and 0.78 Å near the Re and O(2) atoms, respectively. Atomic scattering factors and anomalous dispersion terms were as in SHELXL 93.[16] The drawings were made with ORTEP[17] and all the calculations were performed on a 3000 Dec α computer.

CCDC reference number 186/1658.

See http://www.rsc.org/suppdata/dt/1999/3735/ for crystallographic files in .cif format.

Results and discussion

Syntheses of the complexes and spectroscopic data

The complex [ReO{κ^3-B(pz)$_4$}(OMe)$_2$] **1** reacts with pyridine-2-thiol or with 3-trimethylsilylpyridine-2-thiol at room temperature in a 1:1 molar ratio leading to [ReO{κ^2-B(pz)$_4$}(κ^2-Spy*)(OMe)] (Spy* = 2-SC$_5$H$_4$N **2** or 2-SC$_5$H$_3$NSiMe$_3$-3 **3**) (Scheme 1). When the same reaction is carried out at higher temperatures and with an excess of pyridine-2-thiol **1** is almost quantitatively converted into [ReO{κ^3-B(pz)$_4$}(κ^1-2-SC$_5$H$_4$N)$_2$] **4**. With the bulkier 3-trimethylsilylpyridine-2-thiol the bis-thiolate is not formed and a decomposition process occurred; it was not possible to identify any of the products. We also attempted to prepare complex **4** by treating [{ReO(μ-O)[κ^3-B(pz)$_4$]}$_2$][9] with pyridine-2-thiol, but in this case a mixture of species was obtained. One has been identified as **4** and the other, although slightly contaminated, was tentatively formulated as the dimer "[{ReO{κ^2-B(pz)$_4$}(κ^2-2-SC$_5$H$_4$N)$_2$}$_2$(μ-O)]" **5**, based on IR and ^{1}H NMR spectroscopies.

Treating [ReO{κ^2-B(pz)$_4$}(κ^2-2-SC$_5$H$_4$N)(OMe)] **2** and [ReO{κ^2-B(pz)$_4$}(κ^2-2-SC$_5$H$_3$NSiMe$_3$-3)(OMe)] **3** with an excess of ClSiMe$_3$ the oxochloride derivatives [ReO{κ^3-B(pz)$_4$}(κ^1-2-SC$_5$H$_4$N)Cl]·HCl **6** and [ReO{κ^3-B(pz)$_4$}Cl$_2$] were obtained, respectively. The different results found for compounds **2** and **3** are certainly accounted for by the presence of the bulky SiMe$_3$ group in the pyridine ring (**3**), which seems to disfavor the formation of complexes containing κ^3-B(pz)$_4$, due to an increase of repulsive interactions.

The conversion of [ReO{κ^2-B(pz)$_4$}(κ^2-2-SC$_5$H$_4$N)(OMe)] **2** into [ReO{κ^3-B(pz)$_4$}(κ^1-2-SC$_5$H$_4$N)Cl]·HCl **6** involves the replacement of the methoxide and a haptotropic shift of the bidentate B(pz)$_4$ and Spy* ligands from κ^2 to κ^3 and from κ^2 to κ^1, respectively. These results contrast with others previously reported for the analogous [ReO{κ^2-B(pz)$_4$}(L–L)-(OMe)] (L–L = acetylacetonate, quinolin-8-olate).[10] In fact,

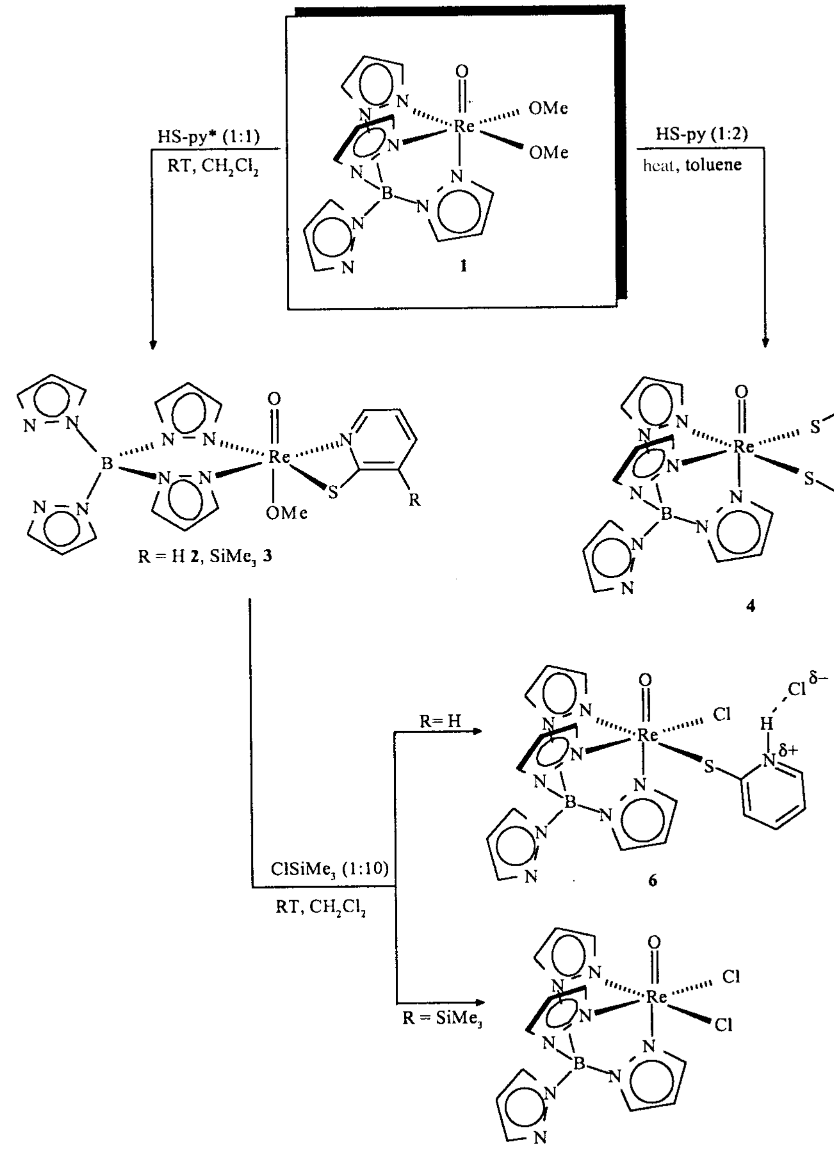

Scheme 1

these complexes react with ClSiMe$_3$ leading to [ReO{κ^2-B(pz)$_4$}(L–L)Cl], with retention of the κ^2 co-ordination mode of the B(pz)$_4$ ligand and with co-ordination of the oxygen atom of acetylacetonate and quinolin-8-olate *trans* to the Re=O core. The difference found can be explained by the better π donor character of acetylacetonate and quinolin-8-olate, compared to pyridine-2-thiolate, which favour the co-ordination of the oxygen atoms of these ligands *trans* to the oxo group.

The IR spectra of complexes **2**–**6** show medium to strong bands in the 945–970 cm^{-1} range, assigned to ν(Re=O) stretching vibrations, and lower frequencies were observed for **2** and **3**, which contain the *trans*-[ReO(OMe)]$^{2+}$ unit. The competition of the methoxide group for π bonding with the d$_\pi$ orbitals of the metal explains the weakness of the rhenium–oxygen bond. The presence of the methoxide group in **2** and **3** was confirmed by a strong and medium ν(Re–OMe) stretching band at 514 and 510 cm^{-1}, respectively. In the spectrum of complex **5** a strong stretching band appears at 680 cm^{-1}, which is not due to the presence of the B(pz)$_4$ and S-py ligands, since it is absent in the IR spectra of **3**, **4** and **6**. We have assigned this band to ν(Re–O–Re), by comparison with the values found for such stretching vibration in the IR spectra of structurally characterized dimeric rhenium(V) oxo complexes containing κ^2 -B(pz)$_4$.[10]

The ^{1}H NMR spectra of complexes [ReO{κ^2-B(pz)$_4$}(κ^2-Spy*)(OMe)] (Spy* = 2-SC$_5$H$_4$N **2** or 2-SC$_5$H$_3$NSiMe$_3$-3 **3**) and "[{ReO[κ^2-B(pz)$_4$](κ^2-2-SC$_5$H$_4$N)$_2$}$_2$(μ-O)]" **5** present a pattern which indicates a κ^2 co-ordination mode for the B(pz)$_4$ ligand (two resonances due to H(3/5) protons of the pyrazolyl rings are high field shifted) and indicates also the magnetic non-equivalence of the pyrazolyl rings (1 : 1 : 1 : 1 pattern). These results are consistent with the C_1 symmetry expected for these complexes and confirmed by the X-ray crystallographic analysis of **3** (see below). However, the complex formulated as **5** was always slightly contaminated and, unfortunately, no crystals suitable for X-ray crystallographic analysis could be obtained. Nevertheless, its IR spectrum is consistent with a dimeric species, as discussed above, and the NMR data indicate a κ^2 co-ordination mode for B(pz)$_4$ and a C_1 symmetry around the metal center. These spectroscopic data are not sufficient to distinguish between the **5a** and **5b** structures depicted, which have been previously found in other dimeric rhenium(V) oxo complexes containing κ^2-B(pz)$_4$ and other monoanionic and bidentate co-ligands.[10]

Complexes [ReO{κ^3-B(pz)$_4$}(κ^1-2-SC$_5$H$_4$N)$_2$] **4** and [ReO{κ^3-B(pz)$_4$}(κ^1-2-SC$_5$H$_4$N)Cl]·HCl **6** present, at room temperature, ^{1}H NMR spectra which indicate the presence of κ^3-B(pz)$_4$ (only the H(4) protons of the pyrazolyl rings are high field shifted). In the ^{1}H NMR spectrum of **6** the pattern observed for the resonances of the protons of the pyrazolyl rings (1 : 1 : 1 : 1) is also consistent with the C_1 symmetry expected for the molecule and found in the solid state by X-ray diffraction analysis (see below). The pyridinium proton involved in the hydrogen

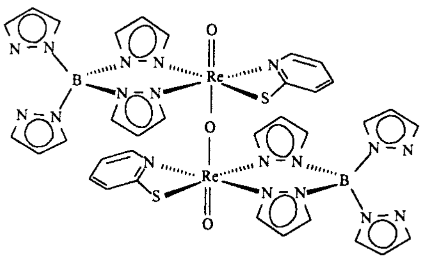

5a

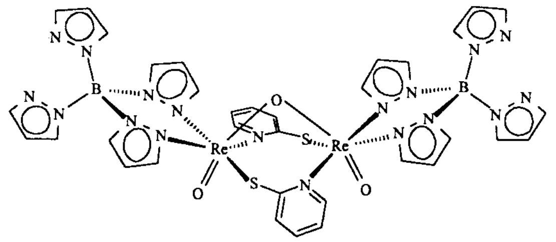

5b

bond interaction N–H · · · Cl was also found in the NMR spectrum, appearing as a broad resonance at δ 18.46, a value which compares with the ones reported for hydrogen bonded pyridine acid complexes.[18]

At room temperature the ^{1}H NMR spectrum of complex **4** presents, for the protons of the pyrazolyl rings (2 : 1 : 1) and for the protons of the pyridine-2-thiolate ligands, patterns consistent with a C_s symmetry for the molecule in solution, but the resonances are very broad and no coupling constants could be assigned. These data suggested some dynamic process in solution and this prompted us to run variable temperature ^{1}H NMR studies. In fact, by raising the temperature the resonances due to the H(4), H(3) and H(5) protons of the pyrazolyl rings broadened, collapsed and at 60 °C only one resonance, of intensity four, was observed for each of those protons (see Fig. 1). The resonances due to the two pyridinethiolate ligands were not affected by the temperature, maintaining at 60 °C a pattern consistent with their magnetic equivalence, as observed at 20 °C. For temperatures lower than 20 °C a different situation was observed. At −80 °C the spectrum showed 17 resonances, one integrating for three protons, another for two protons and the remaining 15 resonances integrating for one proton each. Assuming the occasional overlapping of some resonances, we can say that this pattern for the protons of the pyrazolyl rings (1 : 1 : 1 : 1) and for the protons of the pyridine-2-thiolate ligands indicates the non equivalence of the Spy* ligands and of the pyrazolyl rings of B(pz)$_4$.

As suspected, these studies confirmed a fluxional behaviour for complex **4**, and indicate that most probably there are two dynamic processes involved. At higher temperature, the magnetic equivalence of all the pyrazolyl rings can be explained by the de-co-ordination/rotation/co-ordination of the pyrazolyl rings of B(pz)$_4$, and this is certainly induced by the *trans* effect of the oxo ligand, as we suggested previously for other fluxional complexes with the moiety [ReO{κ^3-B(pz)$_4$}]$^{2+}$.[9,11] At lower temperatures the free rotation of the pyridine-2-thiolate ligands around the Re–S bond is hindered and results in the C_1 symmetry of the molecule. Probably, the B(pz)$_4$ ligand remains κ^3 co-ordinated, as found in the solid state crystal structure of **4** (see below).

Molecular structures of complexes 3, 4 and 6

The structures of complexes [ReO{κ^2-B(pz)$_4$}(κ^2-2-SC$_5$H$_3$-NSiMe$_3$-3)(OMe)] **3**, [ReO{κ^3-B(pz)$_4$}(κ^1-2-SC$_5$H$_4$N)$_2$] **4** and [ReO{κ^3-B(pz)$_4$}(κ^1-2-SC$_5$H$_4$N)Cl]·HCl **6** consist of discrete mononuclear units with the rhenium atom in a distorted octahedral environment. The ORTEP views of the structures are shown in Figs. 2–4, and selected bond distances and angles are listed in Tables 2–4, respectively.

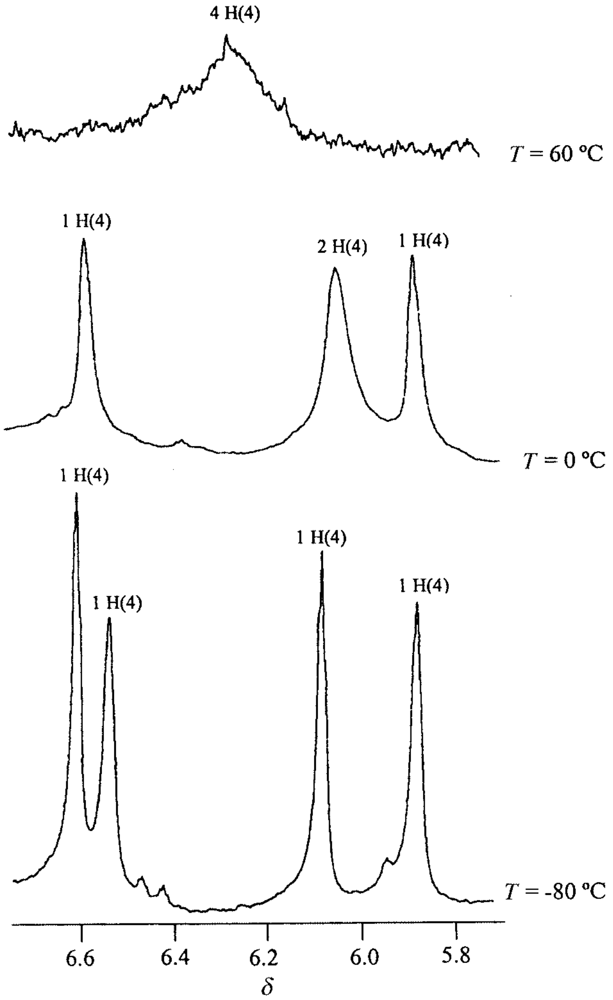

Fig. 1 Variable temperature ^{1}H NMR spectra (in the H(4) region) for complex **3**.

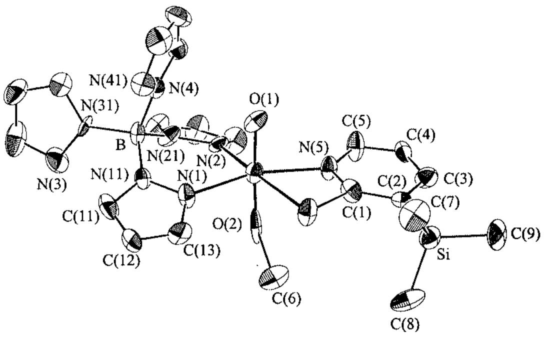

Fig. 2 An ORTEP drawing of complex **3** with the atom numbering scheme. Thermal ellipsoids in all the structures are drawn at the 40% probability level.

The Re–O(1) bond distances (1.646(13) in **3**, 1.690(5) in **4**, 1.673(6) Å in **6**) are in the range found for other octahedral rhenium(V) monooxo complexes containing κ^2 or κ^3-B(pz)$_4$.[8–11] For complex **3** the rhenium–methoxide bond is characterized by an unusually short Re–O(2) bond distance (1.78(2) Å) which we cannot explain, and consequently a comparison with the values observed for other complexes with the moiety *trans*-[ReO(OMe)]$^{2+}$ is inappropriate.[10,19–21]

The tetrakis(pyrazolyl)borate is bidentate in complex **3** and occupies two equatorial positions, while in **4** and **6** it is tridentate, occupying a face of the distorted octahedron. In **3** the 3-trimethylsilylpyridine-2-thiolate ligand is bidentate, through

Table 1 Crystallographic data for complexes **3**, **4** and **6**

	3	**4**·HSC_5H_4N	**6**·CH_2Cl_2
Formula	$C_{21}H_{27}BN_9O_2ReSSi$	$C_{22}H_{20}BN_{10}OReS_2 \cdot C_5H_5NS$	$C_{17}H_{17}BCl_2N_9OReS \cdot CH_2Cl_2$
M	694.68	812.77	748.29
Crystal system	Monoclinic	Monoclinic	Triclinic
Space group	$P2_1/c$ (no. 14)	$P2_1/n$ (no. 14)	$P\bar{1}$ (no. 2)
a/Å	17.545(3)	10.419(1)	8.5130(6)
b/Å	8.2966(9)	25.297(2)	9.1937(8)
c/Å	19.997(3)	11.582(1)	16.678(2)
α/°	—	—	80.472(9)
β/°	110.91(1)	94.35(2)	81.748(9)
γ/°	—	—	89.193(6)
U/Å^3	2719.1(7)	3043.9(5)	1273.9(2)
Z	4	4	2
T/K	293	293	293
μ(Mo-Kα)/mm^{-1}	4.626	4.242	5.303
No. reflections measured	4418	6704	4612
No. unique reflections (R_{int})	4263 (0.0471)	6366 (0.1148)	4446 (0.0223)
$R1^a$	0.0750	0.0507	0.0481
$wR2^a$	0.1358	0.0747	0.0937

[a] Calculated for data with $I > 2\sigma(I)$ only.

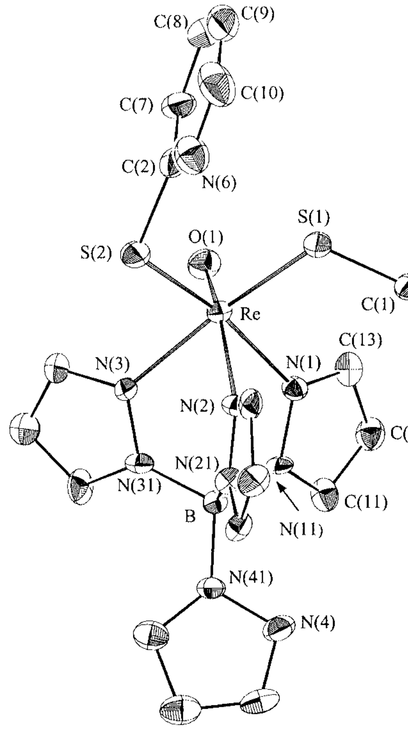

Fig. 3 An ORTEP drawing of complex **4** with the atom numbering scheme.

the sulfur and nitrogen atoms, occupying two equatorial positions. In contrast, in **4** and **6** the pyridine-2-thiolate ligands are monodentate through the sulfur atom, occupying two or one equatorial position, respectively. The Re–S bond distance of 2.424(5) Å in complex **3** is significantly larger than the values found for the rhenium–sulfur distances in **4** (2.309(2) and 2.313(2) Å) and **6** (2.337(3) Å). The long Re–S bond distance found in **3** is easily justified by the chelate co-ordination mode of the pyridinethiolate ligand and by the steric constraints imposed by co-ordination of the sp^2 hybridized pyridyl nitrogen.[5] Such steric constraints are also responsible for the small chelate angle N(5)–Re–S of 66.9(4)° found in **3**, compared with the angles S(1)–Re–S(2) (88.06(8)°) and Cl(1)–Re–S (90.22(10)°) observed for **4** and **6**, respectively. The rhenium–sulfur bond distances found for **4** and **6** compare with ones found previously in other rhenium(V) oxo complexes containing thiolate ligands.[9,22,23]

In the X-ray diffraction analysis of complex **4** one molecule of pyridine-2-thiol of crystallization per asymmetric unit was found. The successful location and refinement of an hydrogen atom 0.85 Å from N(1A) confirmed that the molecule of crystallization is in the thione form. Consistently, the C(1A)–S(1A) bond distance of 1.680(9) Å is shorter than the average C–S bond distance (1.78(1) Å) found for the unidentate pyridine-2-thiolate ligands bound to rhenium in complexes **4** and **6**. The N–H proton of the thione is hydrogen bonded to an unco-ordinated nitrogen atom of one of the pyridine-2-thiolate ligands co-ordinated to the metal (N(1A)···N(5′) 2.97; H(1A)···N(5) 2.13 Å; N(1A)–H···N(5) 170.3°). This hydrogen bonding interaction has structural parameters similar to the ones described for the compound $[Sn(\kappa^2\text{-}2\text{-}SC_5H_4N)_2(\kappa^1\text{-}2\text{-}SC_5H_4N)_2]\cdot C_5H_5NS$, for which a similar hydrogen bond interaction has also been confirmed by X-ray diffraction analysis.[24]

Table 2 Selected bond distances [Å] and angles [°] for complex **3**

Re–O(1)	1.646(13)	Re–O(2)	1.78(2)
Re–N(1)	2.11(2)	Re–N(2)	2.141(14)
Re–N(5)	2.140(14)	Re–S	2.424(5)
S–C(1)	1.76(2)	O(2)–C(6)	1.45(2)
O(1)–Re–O(2)	177.0(6)	O(1)–Re–N(1)	96.7(6)
O(2)–Re–N(1)	86.3(6)	O(1)–Re–N(5)	93.1(6)
O(2)–Re–N(5)	83.9(6)	N(1)–Re–N(5)	164.9(6)
O(1)–Re–N(2)	95.9(6)	N(1)–Re–N(2)	87.3(6)
N(5)–Re–N(2)	103.1(5)	O(1)–Re–S	92.7(4)
O(2)–Re–S	86.2(4)	N(1)–Re–S	101.1(4)
N(5)–Re–S	66.9(4)	N(2)–Re–S	167.2(4)
C(6)–O(2)–Re	149.7(13)	C(1)–N(5)–C(5)	120(2)

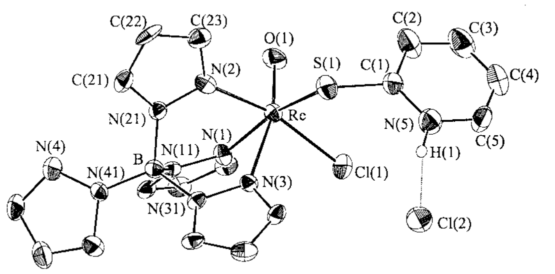

Fig. 4 An ORTEP drawing of complex **6** with the atom numbering scheme. The hydrogen atom H(1) is represented as a circle of arbitrary radius.

As discussed above, the ^1H NMR of $[ReO\{\kappa^3\text{-}B(pz)_4\}(\kappa^1\text{-}2\text{-}SC_5H_4N)Cl]\cdot HCl$ **6** is also consistent with protonation of the unco-ordinated nitrogen of the pyridine-2-thiolate ligand. The X-ray analysis allowed the location and isotropic refinement of

Table 3 Selected bond distances [Å] and angles [°] for complex **4**

Re–O(1)	1.690(5)	Re–N(1)	2.169(6)
Re–N(2)	2.220(6)	Re–N(3)	2.150(6)
Re–S(1)	2.309(2)	Re–S(2)	2.313(2)
S(1)–C(1)	1.782(8)	S(2)–C(2)	1.790(9)
S(1A)–C(1A)[a]	1.680(9)		
S(1)–Re–S(2)	88.06(8)	S(2)–Re–N(1)	166.2(2)
O(1)–Re–S(1)	104.6(2)	S(2)–Re–N(2)	88.6(2)
O(1)–Re–S(2)	104.3(2)	S(2)–Re–N(3)	85.5(2)
O(1)–Re–N(1)	88.2(2)	N(1)–Re–N(2)	78.0(2)
O(1)–Re–N(2)	161.7(2)	N(1)–Re–N(3)	88.5(2)
O(1)–Re–N(3)	91.1(3)	N(2)–Re–N(3)	76.9(2)
S(1)–Re–N(1)	94.5(2)	S(1)–Re–N(2)	88.5(2)
S(1)–Re–N(3)	164.1(2)	Re–S(1)–C(1)	111.3(3)
Re–S(2)–C(2)	109.9(3)	C(1)–N(5)–C(6)	117.3(7)
C(2)–N(6)–C(10)	115.2(9)	C(1A)–N(1A)–C(5A)[a]	124.3(8)

[a] For pyridine-2-thiol of solvation.

Table 4 Selected bond distances [Å] and angles [°] for complex **6**

Re–O(1)	1.673(6)	Re–N(1)	2.073(8)
Re–N(2)	2.099(8)	Re–N(3)	2.250(7)
Re–Cl(1)	2.335(3)	Re–S	2.337(3)
S–C(1)	1.771(10)		
O(1)–Re–N(1)	93.6(3)	O(1)–Re–N(2)	90.6(3)
N(1)–Re–N(2)	89.3(3)	O(1)–Re–N(3)	165.5(3)
N(1)–Re–N(3)	78.6(3)	N(2)–Re–N(3)	77.2(3)
O(1)–Re–Cl(1)	104.4(2)	N(1)–Re–Cl(1)	86.8(2)
N(2)–Re–Cl(1)	164.7(2)	N(3)–Re–Cl(1)	87.5(2)
O(1)–Re–S	102.1(3)	N(1)–Re–S	164.3(2)
N(2)–Re–S	89.6(2)	N(3)–Re–S	85.9(2)
Re–S–C(1)	105.7(4)	Cl(1)–Re–S	90.22(10)
C(1)–N(5)–C(5)	121.8(1)		

the hydrogen atom, with a N(5)–H(1) bond distance of 1.0 Å. The protonation of N(5) is consistent with the angle C(1)–N(5)–C(5) of 121.8(1)°, since protonated and non-protonated nitrogen atoms of pyridine rings have angles greater or less than 120°, respectively. The H(1) proton is involved in a strong hydrogen bonding interaction with the unco-ordinated chloride (N(5)···Cl(2) 2.973; H(1)···Cl(2) 1.99 Å; N(5)–H···Cl(2) 165.9°). The distance N(5)–Cl(2) is at the short end of the range of lengths reported for N–H···Cl hydrogen bonds.[25]

Concluding remarks

We have shown that the introduction of the bulky $SiMe_3$ group in the 3 position of pyridine-2-thiolate disfavors tripodal co-ordination of poly(pyrazolyl)borate, most probably as a consequence of steric constraints. We have also demonstrated that the hapticities of $B(pz)_4$ and Spy* ligands can be switched by the introduction of unidentate co-ligands with different electronic properties. Our results suggest the concomitant influence of electronic and steric factors in the chemistry of rhenium(V) oxo complexes containing the ambivalent $B(pz)_4$ and Spy* ligands.

References

1 H. Spies, T. Fietz, H. J. Pietzsch, B. Johanssen, P. Leibnitz, G. Reck, D. Scheller and K. Klostermann, *J. Chem. Soc.*, *Dalton Trans.*, 1995, 2277.

2 M. Papadopoulos, C. Tsoukala, I. Pirmettis, B. Nock, T. Maina, Z. Abedin, C. P. Raptopoulou, A. Terzis and E. Chiotellis, *Inorg. Chim. Acta*, 1999, **285**, 97.

3 K. P. Maresca, G. H. Bonavia, J. W. Babich and J. Zubieta, *Inorg. Chim. Acta*, 1999, **284**, 252.

4 D. J. Rose, K. P. Maresca, T. Nicholson, A. Davison, A. G. Jones, J. Babich, A. Fischman, W. Graham, J. R. D. DeBord and J. Zubieta, *Inorg. Chem.*, 1998, **37**, 2701.

5 D. J. Rose, K. P. Maresca, P. B. Kettler, Y. D. Chang, V. Soghomomian, Q. Chen, M. J. Abrams, S. K. Larsen and J. Zubieta, *Inorg. Chem.*, 1996, **35**, 3548.

6 P. B. Kettler, Y. Chang, D. Rose, J. Zubieta and M. J. Abrams, *Inorg. Chim. Acta*, 1996, **244**, 199.

7 A. Domingos, J. Marçalo, A. Paulo, A. Pires de Matos and I. Santos, *Inorg. Chem.*, 1993, **32**, 5114.

8 A. Paulo, A. Domingos, A. Pires de Matos, I. Santos, M. F. N. N. Carvalho and A. J. L. Pombeiro, *Inorg. Chem.*, 1994, **33**, 4729.

9 A. Paulo, A. Domingos, J. Marçalo, A. Pires de Matos and I. Santos, *Inorg. Chem.*, 1995, **34**, 2113.

10 A. Paulo, A. Domingos and I. Santos, *Inorg. Chem.*, 1996, **35**, 1798.

11 D. Nunes, A. Domingos, L. Patrício, A. Paulo, I. Santos, M. F. N. N. Carvalho and A. J. L. Pombeiro, *Inorg. Chim. Acta*, 1998, **271**, 65.

12 A. Paulo, A. Domingos and I. Santos, *Inorg. Chem.*, 1998, **37**, 6807.

13 E. Block, M. Gernon, H. Kang, G. Ofori-Okai and J. Zubieta, *Inorg. Chem.*, 1991, **30**, 1736.

14 C. K. Fair, MOLEN, Enraf-Nonius, Delft, 1990.

15 G. M. Sheldrick, SHELXS 86, Program for the Solution of Crystal Structure, University of Göttingen, 1986.

16 G. M. Sheldrick, SHELXS 93, Program for the Refinement of Crystal Structure, University of Göttingen, 1993.

17 C. K. Johnson, ORTEP II, Report ORNL-5138, Oak Ridge National Laboratory, Oak Ridge, TN, 1976; P. McArdle, *J. Appl. Crystallogr.*, 1995, **28**, 65.

18 N. S. Gobulev, I. G. Shendervich, S. N. Smirnov, G. S. Denisov and H. H. Limbach, *Chem. Eur. J.*, 1999, **5**, 492.

19 A. Paulo, J. Ascenso, A. Domingos, A. Galvão and I. Santos, *J. Chem. Soc.*, *Dalton Trans.*, 1999, 1798.

20 G. F. Ciani, G. D'Alfonso, P. F. Romiti, A. Sironi and M. Freni, *Inorg. Chim. Acta*, 1983, **72**, 29.

21 S. Abram, U. Abram, E. Schulz-Lang and J. Strahle, *Acta Crystallogr.*, *Sect. C*, 1995, **51**, 1078.

22 I. A. Degnan, J. Behm, M. R. Cook and W. A. Herrmann, *Inorg. Chem.*, 1998, **37**, 6807.

23 P. B. Kettler, Y. D. Chang, Q. Chen, J. Zubieta, M. J. Abrams and S. K. Larsen, *Inorg. Chim. Acta*, 1995, **231**, 13.

24 L. C. Damude, P. A. W. Dean, V. Manivannan, R. S. Srivastava and J. J. Vitall, *Can. J. Chem.*, 1990, **68**, 1323.

25 S. M. Redmore, C. E. F. Rickard, S. J. Webb and L. J. Wright, *Inorg. Chem.*, 1997, **36**, 4743.

Paper 9/05911C